Broadband multilayer mirrors for optimum use of soft x-ray source output

2000 J. Opt. A: Pure Appl. Opt. 2 452

(http://iopscience.iop.org/1464-4258/2/5/317)

J. Opt. A: Pure Appl. Opt. **2** (2000) 452–457. Printed in the UK PII: S1464-4258(00)13814-0

Broadband multilayer mirrors for optimum use of soft x-ray source output

Z Wang†‡ and A G Michette†

† Department of Physics, King's College London, Strand, London WC2R 2LS, UK
‡ State Key Laboratory of Applied Optics, Changchun Institute of Optics and Fine Mechanics, Chinese Academy of Sciences, PO Box 1024, Changchun 130022, People's Republic of China

Received 9 May 2000

Abstract. A method of designing soft x-ray multilayer mirrors which maximize the throughput of a system in a given wavelength range is described, where throughput is defined as the product of multilayer reflectivity and source spectral intensity. It is shown that the method can also be used to obtain a flat throughput response in the required wavelength range, and that in either case mirrors which suppress the throughput outside the desired range can be designed. The method is used to optimize multilayers for the wavelength range 13–19 nm, with suppressed throughput in the ranges 12–13 and 19–25 nm. In the latter case the ratio of intensities inside and outside 13–19 nm can be increased from 0.91 to 131 and from 0.70 to 35 for two different source spectra and maximized throughput, or to 67 and 25 for flat throughput.

Keywords: Depth-graded multilayer mirrors, soft x-ray optics, broadband x-ray optics

1. Introduction

In previous papers the designs of depth-graded x-ray multilayer mirrors with broad angular [1] or broad wavelength [2] responses were described; references to earlier work on this subject are given in these two papers. The method used was a stochastic one in which, starting from a particular layer distribution (which could either be a periodic multilayer or the results of a previous calculation), the position of a random boundary was shifted by a random amount. If this resulted in the improvement of some merit function the change was kept; otherwise it was rejected. This process was continued until the merit function was optimized.

The merit functions that were used, for single-mirror systems, were

$$\mathrm{MF} = \int_{\eta_{\min}}^{\eta_{\max}} R(\eta)\,\mathrm{d}\eta \tag{1}$$

for maximizing the reflectivity $R(\eta)$ in a given range of glancing angle ($\eta = \theta$) or wavelength ($\eta = \lambda$), and

$$\mathrm{MF} = \int_{\eta_{\min}}^{\eta_{\max}} [R(\eta) - R_0]^2\,\mathrm{d}\eta \tag{2}$$

for obtaining a flat response over the range, with a target reflectivity of R_0. The choice of R_0 is an important part of the optimization process, as if it is too large the target may not be achieved. In either case, the influence of interlayer roughness, random or systematic boundary position errors and non-sharp boundaries could be taken into account, so that the multilayers could be designed with manufacturing tolerances in mind.

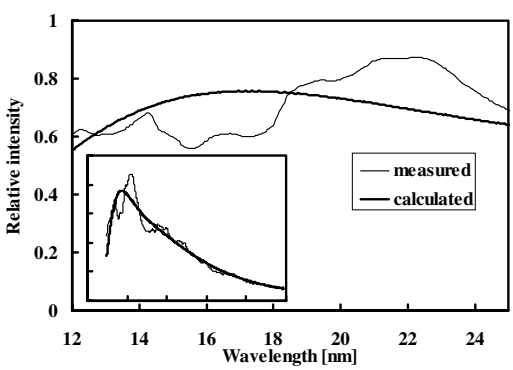

Figure 1. The measured and calculated (bremsstrahlung) emission spectra of a laser-plasma source with a rhenium target. The main figure shows the spectra in the wavelength range 12–25 nm, as used in the modelling of sections 2–5, and the inset shows the emission over the range 0–100 nm.

The mirrors designed using these merit functions had good calculated performances, but did not take into account the x-ray spectrum incident on the multilayer. This may be important in an application since, for example, the requirement may be for maximum or flat throughput (mirror reflectivity times source spectrum) in a given range, perhaps coupled with minimum throughput outside that range (the selectivity). These problems are addressed in this paper by

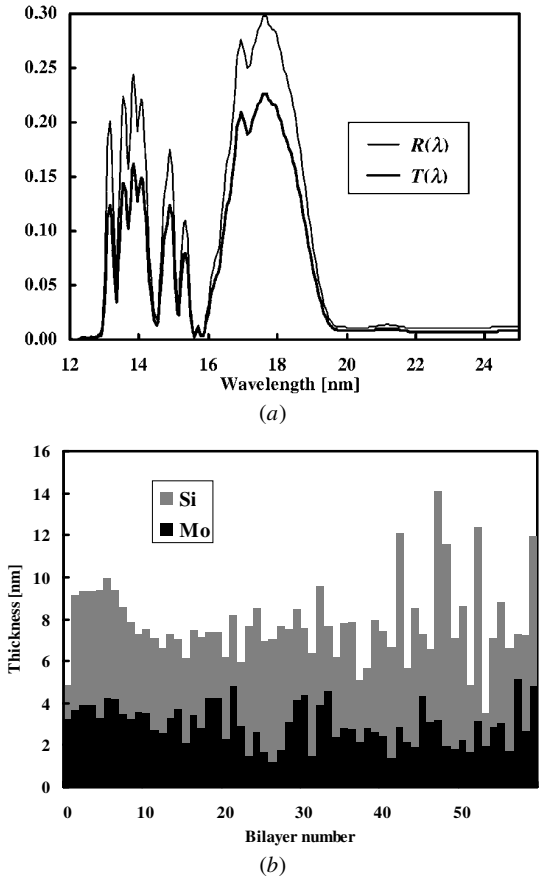

Figure 2. (*a*) The reflectivity and throughput of an Mo/Si multilayer (M1) optimized for maximum throughput in the wavelength range 13–19 nm using the calculated source spectrum. (*b*) The corresponding distribution of layer thicknesses, with bilayer number increasing downwards from the top of the multilayer stack. The local period is given by the total height of each histogram bar, and the local silicon thickness by the difference between the total height and the molybdenum height.

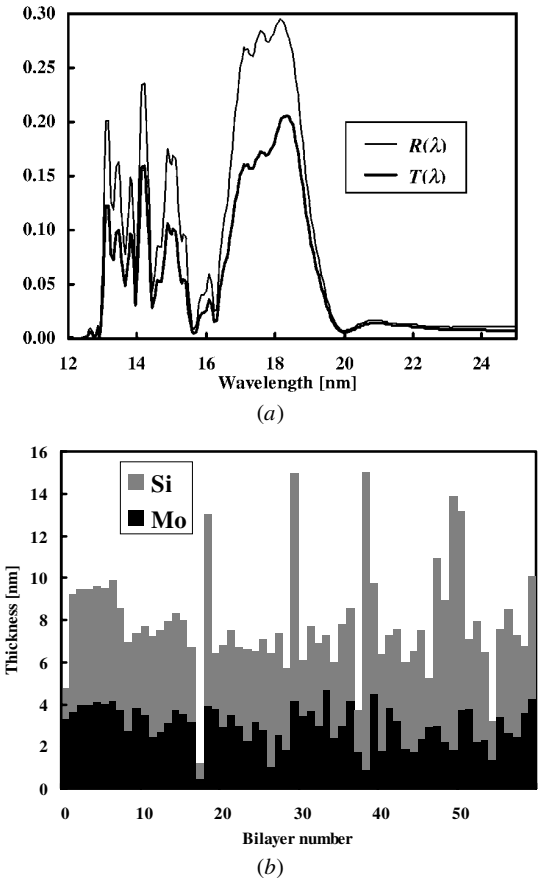

Figure 3. (*a*) The reflectivity and throughput of an Mo/Si multilayer (M2) optimized for maximum throughput in the wavelength range 13–19 nm using the measured source spectrum. (*b*) The corresponding distribution of layer thicknesses, with bilayer number increasing downwards from the top of the multilayer stack. The local period is given by the total height of each histogram bar, and the local silicon thickness by the difference between the total height and the molybdenum height.

the specification of suitable merit functions.

In section 2 of this paper the technique is applied to optimize an Mo/Si depth-graded multilayer for maximum throughput at normal incidence in the wavelength range 13–19 nm using two source functions. One is the measured spectrum of a laser-plasma source with a rhenium target [3], and the other is the calculated bremsstrahlung emission of the same set-up, normalized to the same integrated emission in the wavelength range up to 100 nm. This type of source can be used, e.g., for projection EUV lithography in the wavelength range ∼13–19 nm [4] and for soft x-ray fluorescence analysis [5]. The two spectra are shown in figure 1; the calculated spectrum has an intensity ratio $I(13\text{–}19\,\text{nm})/[I(12\text{–}13\,\text{nm})+I(19\text{–}25\,\text{nm})]$ of 0.91 while for the measured spectrum this is 0.70. An optimization coupling maximum throughput in the range 13–19 nm with minimum throughput outside that range is presented in section 3.

The same wavelength range and spectra are used in sections 4 and 5, respectively, for similar multilayers with a flat throughput and a flat throughput coupled with minimum throughput at shorter and longer wavelengths. Unless otherwise stated an interfacial roughness of 0.3 nm and zero boundary position errors are assumed, and the boundaries are assumed to be sharp since experimentally achievable tolerances do not have major effects [2]. In all the calculations the top layer of the stack is silicon, which is the case for manufactured multilayers to prevent oxidization.

All the examples discussed in this paper are for the wavelength responses of depth-graded multilayer mirrors. Clearly, the method could also be applied to the angular response.

2. High throughput multilayer

For maximum throughput in a given wavelength range with a source spectrum $S(\lambda)$ the merit function that should be maximized is

$$\text{MF} = \int_{\lambda_{\min}}^{\lambda_{\max}} T(\lambda)\,\mathrm{d}\lambda \tag{3}$$

where $T(\lambda) = R(\lambda)S(\lambda)$ and where, in this calculation, $\lambda_{\min} = 13$ nm and $\lambda_{\max} = 19$ nm. It should be noted that the source spectrum is given in terms of relative intensity, so that the magnitude of the throughput is arbitrary.

The resulting reflectivities and throughputs for the calculated and measured spectra are shown in figures 2(*a*) (mirror M1) and 3(*a*) (mirror M2), respectively, and the

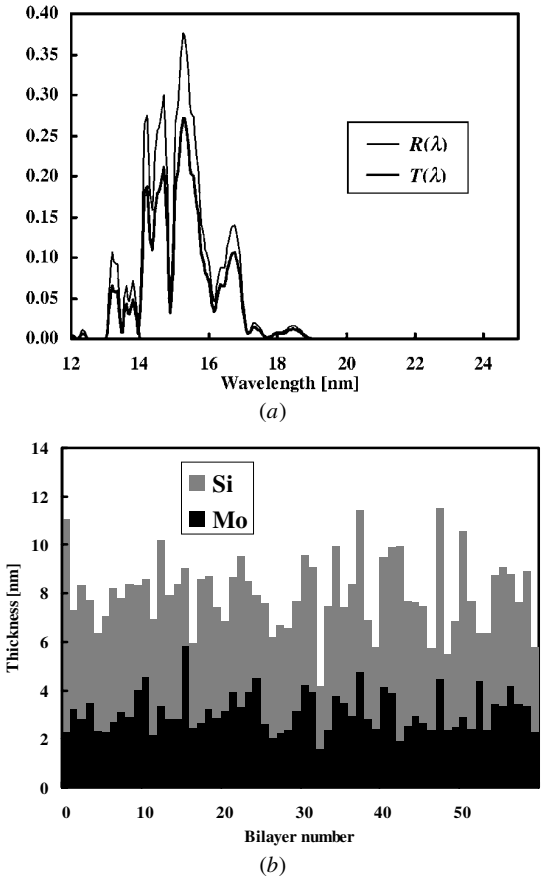

Figure 4. (*a*) The reflectivity and throughput of an Mo/Si multilayer (M3) optimized for maximum throughput in the wavelength range 13–19 nm coupled to minimum throughput outside that range, using the calculated source spectrum. (*b*) The corresponding distribution of layer thicknesses, with bilayer number increasing downwards from the top of the multilayer stack. The local period is given by the total height of each histogram bar, and the local silicon thickness by the difference between the total height and the molybdenum height.

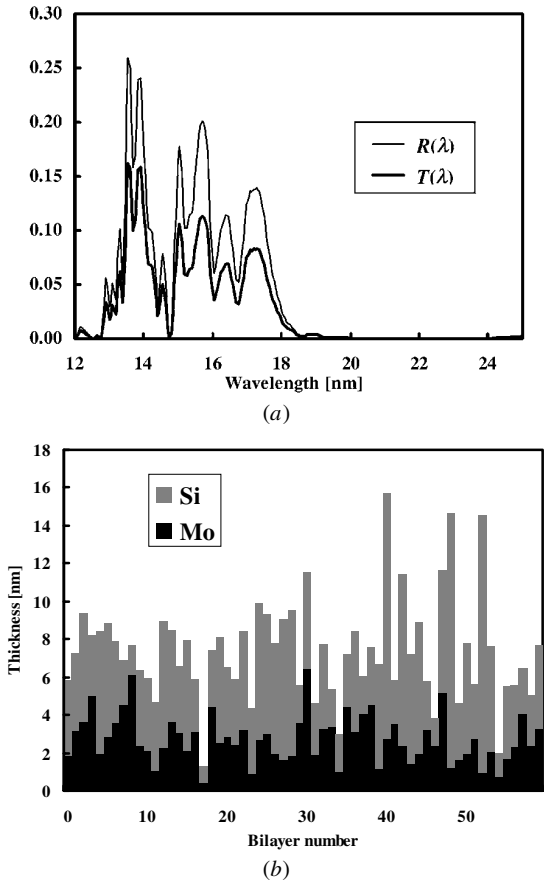

Figure 5. (*a*) The reflectivity and throughput of an Mo/Si multilayer (M4) optimized for maximum throughput in the wavelength range 13–19 nm coupled to minimum throughput outside that range, using the measured source spectrum. (*b*) The corresponding distribution of layer thicknesses, with bilayer number increasing downwards from the top of the multilayer stack. The local period is given by the total height of each histogram bar, and the local silicon thickness by the difference between the total height and the molybdenum height.

corresponding layer thickness distributions in figures 2(*b*) and 3(*b*). It is clear that merely stipulating maximum throughput has resulted in large fluctuations in reflectivity, which may cause problems in practical applications. The average reflectivity and throughput in the range 13–19 nm are $R_{\text{ave}} = 0.159 \pm 0.090$ and $T_{\text{ave}} = 0.116 \pm 0.068$ for the calculated spectrum mirror, and $R_{\text{ave}} = 0.160 \pm 0.088$ and $T_{\text{ave}} = 0.103 \pm 0.059$ for the measured spectrum case. The large (one standard deviation) errors reflect the fluctuations. The selectivities of the mirrors, i.e. the ratio of the throughput in the required range to that outside it (in this case 12–13 and 19–25 nm) are 11 and 7.3 respectively; although the mirrors were not designed for high selectivity these values are given here for comparison with later results.

For both mirrors there is no obvious trend of layer thickness with layer number, although they have a low-thickness top silicon layer. The thicknesses of the silicon (less absorbing) layers also show more fluctuations. The apparently almost periodic nature of these variations for the second mirror, figure 3(*b*), probably has no significance.

3. High throughput in a given wavelength range with high selectivity

For maximum throughput in the wavelength range λ_2–λ_3 coupled with minimum throughput in the ranges λ_1–λ_2 and λ_3–λ_4, where $\lambda_1 < \lambda_2 < \lambda_3 < \lambda_4$, then the merit function

$$\text{MF} = \frac{\int_{\lambda_2}^{\lambda_3} T(\lambda)\,\mathrm{d}\lambda}{\int_{\lambda_1}^{\lambda_2} T(\lambda)\,\mathrm{d}\lambda + \int_{\lambda_3}^{\lambda_4} T(\lambda)\,\mathrm{d}\lambda}, \tag{4}$$

defined above as the selectivity, must be maximized. The reflectivities and throughputs, with $\lambda_1 = 12$ nm, $\lambda_2 = 13$ nm, $\lambda_3 = 19$ nm and $\lambda_4 = 25$ nm, for the two spectra are shown in figures 4(*a*) and 5(*a*) (mirrors M3 and M4). Comparing figure 4(*a*) with 2(*a*), and 5(*a*) with 3(*a*), shows marked decreases in the reflectivities and throughputs outside the range 13–19 nm, as would be expected from adopting the selectivity as the merit function. The mean reflectivities and throughputs in the desired wavelength range have also decreased, to $R_{\text{ave}} = 0.097 \pm 0.060$ and $T_{\text{ave}} = 0.070 \pm 0.042$ for the calculated source spectrum and to $R_{\text{ave}} = 0.092 \pm$

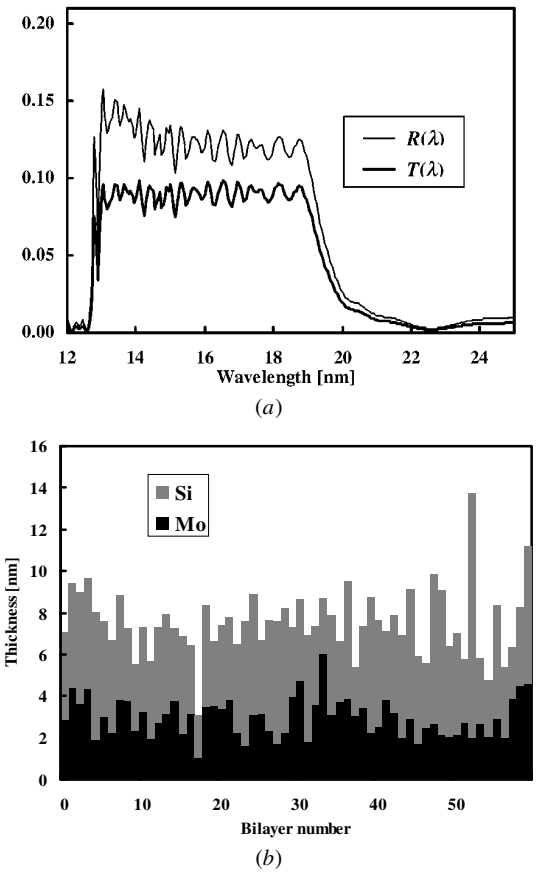

Figure 6. (*a*) The reflectivity and throughput of an Mo/Si multilayer (M5) optimized for flat throughput in the wavelength range 13–19 nm, with a target value of 0.09, using the calculated source spectrum. (*b*) The corresponding distribution of layer thicknesses, with bilayer number increasing downwards from the top of the multilayer stack. The local period is given by the total height of each histogram bar, and the local silicon thickness by the difference between the total height and the molybdenum height.

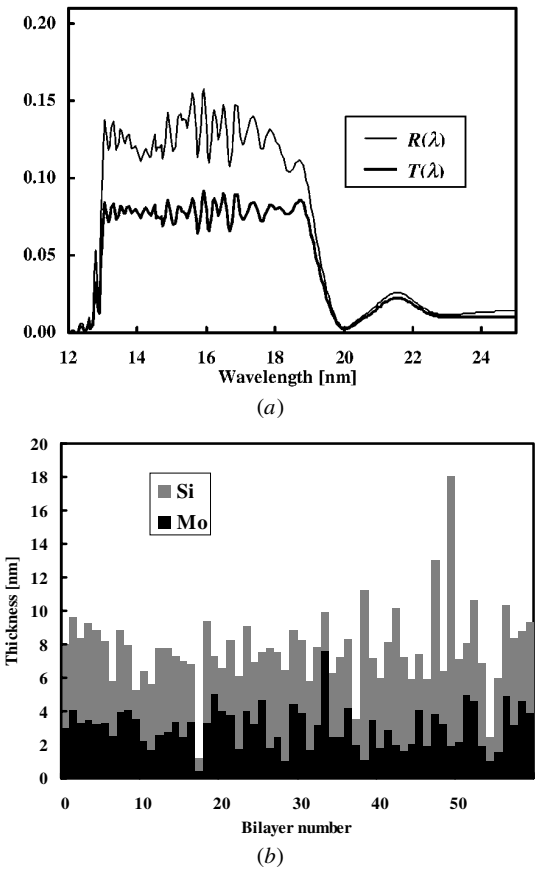

Figure 7. (*a*) The reflectivity and throughput of an Mo/Si multilayer (M6) optimized for flat throughput in the wavelength range 13–19 nm, with a target value of 0.08, using the measured source spectrum. (*b*) The corresponding distribution of layer thicknesses, with bilayer number increasing downwards from the top of the multilayer stack. The local period is given by the total height of each histogram bar, and the local silicon thickness by the difference between the total height and the molybdenum height.

0.065 and $T_{\text{ave}} = 0.056 \pm 0.040$ for the measured spectrum, and the fluctuations are still large. However, the selectivities have increased to 131 and 33 respectively, factors of 145 and 50 higher than the bare spectra. The superior performance in the former case is due to the smoother spectrum and because, as can be seen from figure 1, the calculated spectrum is higher then the measured spectrum in the range 13–19 nm and lower in the ranges 12–13 and 19–25 nm. Again, there are no obvious trends in the layer thickness distributions, figures 4(*b*) and 5(*b*).

4. Flat throughput multilayer

For a flat throughput response in a given wavelength range with a source spectrum $S(\lambda)$ the merit function that should be minimized is

$$\text{MF} = \int_{\lambda_{\min}}^{\lambda_{\max}} [T(\lambda) - T_0]^2 \, \mathrm{d}\lambda \qquad (5)$$

where T_0 is the target value of the throughput in the wavelength range. This merit function was applied to the wavelength range 13–19 nm. The reflectivity and throughput for the calculated source spectrum, with $T_0 = 0.09$ (in arbitrary units), are shown in figure 6(*a*) (mirror M5). The requirement for a flat throughput response has been satisfied; the mean reflectivity and throughput in the 13–19 nm range are $R_{\text{ave}} = 0.125 \pm 0.010$ and $T_{\text{ave}} = 0.0897 \pm 0.0051$, and the selectivity is 5.8. The results for the measured source spectrum, with $T_0 = 0.08$ (chosen lower because of the lower spectrum in this wavelength range), are shown in figure 7(*a*) (mirror M6). Again the throughput response is flat, with the fluctuations in the source spectrum being removed. The mean reflectivity and throughput in the 13–19 nm range are $R_{\text{ave}} = 0.125 \pm 0.013$ and $T_{\text{ave}} = 0.0785 \pm 0.0053$, and the selectivity is 5.0. The corresponding layer thicknesses are shown in figures 6(*b*) and 7(*b*), and again no trend is apparent. However, unlike the previous cases, the thickness distributions for the two source spectra are now similar.

5. Flat throughput in a given wavelength range with high selectivity

If the requirement is for a flat throughput response in the wavelength range λ_2–λ_3 coupled with minimum throughput in the ranges λ_1–λ_2 and λ_3–λ_4, where $\lambda_1 < \lambda_2 < \lambda_3 < \lambda_4$,

Table 1. The performances of the mirrors for the source spectrum for which they were calculated and for the alternative source spectrum.

MF[a]	Mirror	Mean throughput	Selectivity	Mirror	Mean throughput	Selectivity
1	M1	0.116 ± 0.068	11	M2	0.116 ± 0.068	9.3
2	M2	0.103 ± 0.059	7.3	M1	0.102 ± 0.058	8.6
3	M3	0.070 ± 0.042	131	M4	0.066 ± 0.045	45
4	M4	0.056 ± 0.040	35	M3	0.060 ± 0.037	99
5	M5	0.0897 ± 0.0051	5.8	M6	0.090 ± 0.011	6.5
6	M6	0.0785 ± 0.0053	5.0	M5	0.0788 ± 0.0091	4.7
7	M7	0.080 ± 0.021	67	M8	0.088 ± 0.021	24
8	M8	0.077 ± 0.018	25	M7	0.069 ± 0.019	55

[a] 1, maximum throughput, calculated source spectrum; 2, maximum throughput, measured source spectrum; 3, maximum throughput with high selectivity, calculated source spectrum; 4, maximum throughput with high selectivity, measured source spectrum; 5, flat throughput, calculated source spectrum; 6, flat throughput, measured source spectrum; 7, flat throughput with high selectivity, calculated source spectrum; 8, flat throughput with high selectivity, measured source spectrum.

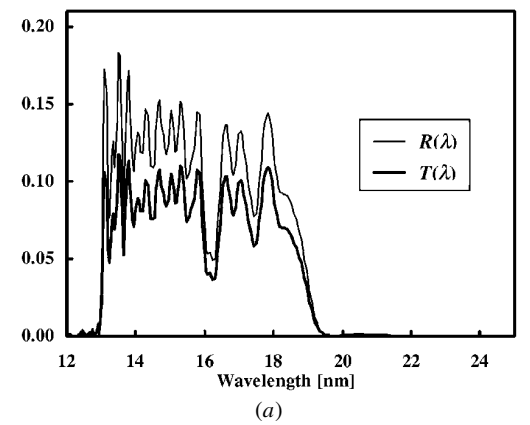

(*a*)

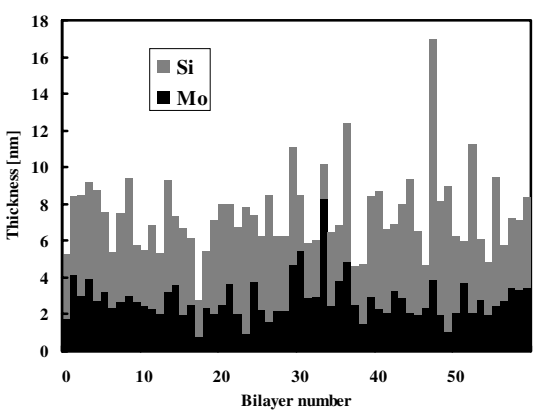

(*b*)

Figure 8. (*a*) The reflectivity and throughput of an Mo/Si multilayer (M7) optimized for flat throughput in the wavelength range 13–19 nm, with a target value of 0.08, coupled with minimum throughput outside that range, using the calculated source spectrum. (*b*) The corresponding distribution of layer thicknesses, with bilayer number increasing downwards from the top of the multilayer stack. The local period is given by the total height of each histogram bar, and the local silicon thickness by the difference between the total height and the molybdenum height.

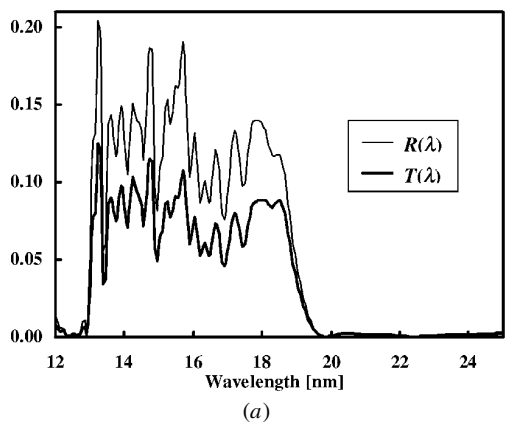

(*a*)

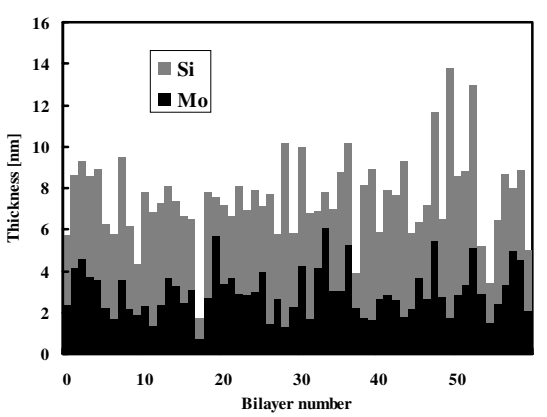

(*b*)

Figure 9. (*a*) The reflectivity and throughput of an Mo/Si multilayer (M8) optimized for flat throughput in the wavelength range 13–19 nm, with a target value of 0.08, coupled with minimum throughput outside that range, using the measured source spectrum. (*b*) The corresponding distribution of layer thicknesses, with bilayer number increasing downwards from the top of the multilayer stack. The local period is given by the total height of each histogram bar, and the local silicon thickness by the difference between the total height and the molybdenum height.

then two merit functions must be minimized simultaneously, namely

$$\mathrm{MF_{in}} = \int_{\lambda_2}^{\lambda_3} [T(\lambda) - T_0]^2 \, \mathrm{d}\lambda \qquad (6)$$

and

$$\mathrm{MF_{out}} = \int_{\lambda_1}^{\lambda_2} T(\lambda) \, \mathrm{d}\lambda + \int_{\lambda_3}^{\lambda_4} T(\lambda) \, \mathrm{d}\lambda. \qquad (7)$$

The reflectivities and throughputs for Mo/Si multilayers

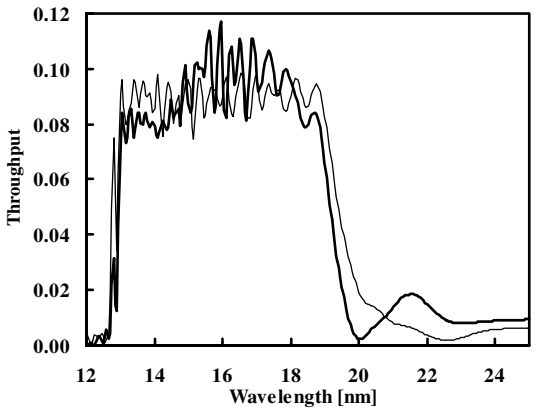

Figure 10. The throughputs of mirrors M5 (light curve) and M6 (heavy curve) for the calculated source spectrum.

with $\lambda_1 = 12$ nm, $\lambda_2 = 13$ nm, $\lambda_3 = 19$ nm and $\lambda_4 = 25$ nm for the calculated and measured source spectra are shown in figures 8(*a*) and 9(*a*) (mirrors M7 and M8), with $T_0 = 0.08$ in each case. Compared with the results of the previous section, the two obvious differences are the lower reflectivities and throughputs outside the desired range, as would be expected, and the greater variability within the range. Less obvious is the more rapid decrease at wavelengths just above 19 nm. For the calculated spectrum the mean reflectivity, throughput and selectivity are 0.110 ± 0.032, 0.080 ± 0.021 and 67, respectively. For the measured spectrum the corresponding values are 0.122 ± 0.031, 0.077 ± 0.018 and 25.

6. Conclusions

The analyses presented above show that it is possible to tailor the structures and performances of depth-graded multilayer mirrors to specific source spectral characteristics, using suitable merit functions. The layer thickness distributions appear to be quite specific to the particular optimization, with differences apparent between the results for the same merit function with different source characteristics. It remains to be seen, therefore, how critical a precise knowledge of the source function is in the design of a particular multilayer. To test this, the throughputs (13–19 nm) and selectivities of each multilayer using the alternative source function have been determined, with the results shown in table 1.

There are some apparent anomalies in table 1. For example, mirror M5, optimized for the calculated source spectrum, has lower throughput and selectivity for that spectrum than does mirror M6, which was optimized for the measured spectrum. However, as can be seen from figure 10, the throughput response of M6 is less flat than that of M5, and flatness was incorporated in the optimization. The same conclusion can be drawn from a comparison between the performances of mirrors M7 and M8. However, this does not explain why mirror M3, designed for maximum throughput with high selectivity using the calculated source spectrum, performs considerably better than mirror M4 when used with the measured source spectrum. Several different calculations of M4, using different starting conditions, lead to the same result, which is thought to be due to better minimization of the throughput outside the selected wavelength range with a smooth (i.e. calculated) source spectrum; as table 1 shows, the throughputs of the two mirrors in the range 13–19 nm are the same within the errors. Another factor to bear in mind in this comparison is that the measured source spectrum (figure 1) is lower in the desired range and higher outside that range than the calculated spectrum.

Apart from these anomalies, it can be seen from table 1 that the mirrors work well for either source spectrum, which indicates that the designs are insensitive to the precise source spectrum. This conclusion holds for a continuum source and may well be different for line sources, which will form the subject of a forthcoming paper, in which the method will be adapted to select given spectral lines and reject others.

Acknowledgment

This study is financially supported in part by the National Natural Science Foundation of China for General Scientific Research, contract no 69778026 to Zhanshan Wang.

References

[1] Wang Z, Cao J and Michette A G 2000 Depth-graded multilayer x-ray optics with broad angular response *Opt. Commun.* **177** 25–32
[2] Michette A G and Wang Z 2000 Optimisation of depth-graded multilayer coatings for broadband reflectivity in the soft x-ray and EUV regions *Opt. Commun.* **177** 47–55
[3] Stuik R 1999 Private communication
[4] Shevelko A P, Shmaenok L A, Churilov S S, Bastiaensen R K F J and Bijkerk F 1998 Extreme ultraviolet spectroscopy of a laser plasma source for lithography *Phys. Scr.* **57** 276–82
[5] Stuik R, Shmaenok L A, Fledderus H, Andreev S S, Shamov E A, Zuev S Y, Salashchenko N N and Bijkerk F 1999 Development of low-energy x-ray fluorescence micro distribution analysis using a laser plasma x-ray source and multilayer optics *J. Anal. At. Spectrosc.* **14** 387–90